

Communication: Light driven remote control of microgels' size in the presence of photosensitive surfactant: Complete phase diagram

Selina Schimka, Yulia D. Gordievskaya, Nino Lomadze, Maren Lehmann, Regine von Klitzing, Artem M. Rumyantsev, Elena Yu. Kramarenko, and Svetlana Santer

Citation: *The Journal of Chemical Physics* **147**, 031101 (2017);

View online: <https://doi.org/10.1063/1.4986143>

View Table of Contents: <http://aip.scitation.org/toc/jcp/147/3>

Published by the [American Institute of Physics](#)

Articles you may be interested in

[Perspective: Photocatalytic reduction of CO₂ to solar fuels over semiconductors](#)

The Journal of Chemical Physics **147**, 030901 (2017); 10.1063/1.4985624

[Communication: Influence of external static and alternating electric fields on water from long-time non-equilibrium ab initio molecular dynamics](#)

The Journal of Chemical Physics **147**, 031102 (2017); 10.1063/1.4994694

[Exploring the free energy gain of phase separation via Markov state modeling](#)

The Journal of Chemical Physics **147**, 034107 (2017); 10.1063/1.4994065

[Photoswitching of azobenzene-containing self-assembled monolayers as a tool for control over silicon surface electronic properties](#)

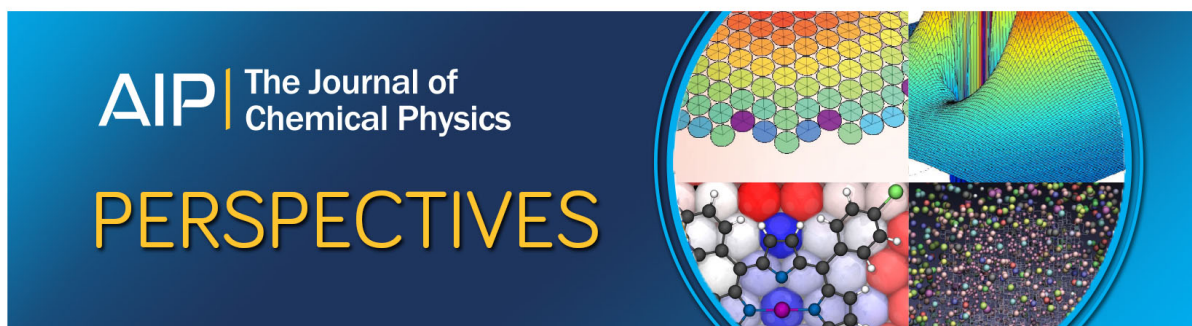
The Journal of Chemical Physics **146**, 104703 (2017); 10.1063/1.4978225

[Selected configuration interaction method using sampled first-order corrections to wave functions](#)

The Journal of Chemical Physics **147**, 034102 (2017); 10.1063/1.4993214

[Cluster expansion of the solvation free energy difference: Systematic improvements in the solvation of single ions](#)

The Journal of Chemical Physics **147**, 034104 (2017); 10.1063/1.4993770



Communication: Light driven remote control of microgels' size in the presence of photosensitive surfactant: Complete phase diagram

Selina Schimka,¹ Yulia D. Gordievskaya,² Nino Lomadze,¹ Maren Lehmann,³ Regine von Klitzing,⁴ Artem M. Rumyantsev,² Elena Yu. Kramarenko,² and Svetlana Santer^{1,a)}

¹*Institute of Physics and Astronomy, University of Potsdam, 14476 Potsdam, Germany*

²*Faculty of Physics, Lomonosov Moscow State University, 119991 Moscow, Russia*

³*Institute of Chemistry, Technical University Berlin, 10623 Berlin, Germany*

⁴*Department of Physics, Technical University Darmstadt, 64287 Darmstadt, Germany*

(Received 2 June 2017; accepted 5 July 2017; published online 18 July 2017)

Here we report on a light triggered remote control of microgel size in the presence of photosensitive surfactant. The hydrophobic tail of the cationic surfactant contains azobenzene group that undergoes a reversible photo-isomerization reaction from a *trans*- to a *cis*-state accompanied by a change in the hydrophobicity of the surfactant. We have investigated light assisted behaviour and the complex formation of the microgels with azobenzene containing surfactant over the broad concentrational range starting far below and exceeding several times of the critical micelle concentration (CMC). At small surfactant concentration in solution (far below CMC), the surfactant in the *trans*-state accommodates within the microgel causing its compaction, while the *cis*-isomer desorbs out of microgel resulting in its swelling. The process of the microgel size change can be described as swelling on UV irradiation (*trans-cis* isomerization) and shrinking on irradiation with blue light (*cis-trans* isomerization). However, at the surfactant concentrations larger than CMC, the opposite behaviour is observed: the microgel swells on blue irradiation and shrinks during exposure to UV light. We explain this behaviour theoretically taking into account isomer dependent micellization of surfactant within the microgels. *Published by AIP Publishing.* [<http://dx.doi.org/10.1063/1.4986143>]

INTRODUCTION

Photosensitive surfactants consisting of a charged head and a hydrophobic tail modified with the azobenzene group have recently attracted extensive experimental and theoretical attention. The broad interest to these substances is stimulated by spectacular practical reason. Indeed, azobenzene containing surfactants allow for photosensitive triggering of any type of charged objects without the need for any irreversible chemical conjugation of these systems with light responsive substances. For instance, one can make polyelectrolyte single chains (DNA, PAA) photosensitive by preparing supramolecular complexes with azobenzene containing surfactants¹⁻⁵ or change plasmonic properties of gold nanoparticles in the presence of either *trans*- or *cis*-isomers of the surfactant.⁶ It is also possible to make polyelectrolyte brushes photo-responsive and thus photo-structured by loading them with oppositely charged photosensitive surfactant.^{7,8} It was also reported that irradiation of a solution of photosensitive surfactant with localized light results in generation of local hydrodynamic flow at the solid/liquid interface relocating particles trapped at this interface.⁹ At the water/air or liquid/liquid interface, the illumination with light results in

a Marangoni type effect intensively utilized in light-driven photofluidics.¹⁰⁻¹⁴

The key mechanism for all these diverse and spectacular applications is the reversible photo-isomerization of azobenzene molecules from the *trans*- to *cis*-state under UV illumination. Two isomers of azobenzene possess different polarity, i.e., the *trans*-state is less polar typically with a dipole moment of ~ 0 D, while *cis*-isomer is highly polar with the dipole moment of ~ 3 D. When azobenzene group is incorporated in a hydrophobic tail of a surfactant molecule, the photo-isomerization changes the hydrophobicity of the whole molecule and thus its solubility. In this way, the critical micelle concentration (CMC) of azobenzene containing surfactants drops several times for the case of *trans*-isomer.¹⁵

This is especially valuable for a recently proposed application of photo-sensitive surfactants for light triggered reversible switching of microgel particles' size.¹⁶⁻¹⁸ When surfactants are added to the aqueous solution of swollen microgels, at a certain concentration there is an essential drop in osmotic pressure due to micellization of surfactants within the gel resulting in microgel particles' collapse and as a consequence its hydrodynamic radius reduces almost two times.¹⁹ This process is reversed during UV irradiation, at which surfactant photoisomerizes to the *cis*-conformation preventing micellization within the gel particles. The *cis*-isomers leave the microgels resulting in re-swelling of the particle back to its initial size. On switching to the *trans*-isomer during irradiation with blue

^{a)} Author to whom correspondence should be addressed: santer@uni-potsdam.de

light, the microgels shrink again. The reversible swelling and shrinkage of the microgels, triggered by periodic changing of the irradiation wave length, occur within seconds.

The surfactant concentration at which microgels shrink is much smaller than its critical micelle concentration (CMC) in solution. Micellization, however, takes place in the interior of the microgel where CMC can be several orders of magnitude smaller.²⁰ In general, until now the complex formation between soft objects such as DNA, polymer brushes, microgels, and azobenzene containing surfactant has been reported at small surfactant concentration, up to two orders of magnitude smaller than its CMC in solution.

Here we report on complex formation of microgels with azobenzene containing surfactant over the broad concentrational range starting far below and exceeding several times that of the CMC. At a larger surfactant concentration, the microgels exhibit opposite behaviour on irradiation: swelling when surfactant is switched to *trans*-conformation (blue irradiation) and shrinkage on UV irradiation. We propose theoretical explanation of this phenomenon as well.

Figure 1 shows the dependence of the microgel size as a function of surfactant concentration and irradiation conditions. The size is presented in a normalized way at which 1 indicates the swollen state in the absence of surfactant. The curve was plotted for the microgels of initial (swollen state) hydrodynamic radius of 600 nm. The surfactant concentration is expressed in values of CMC for surfactants in the *trans*-state. The black line indicates size change in the presence of *trans*-isomers, while the red line depicts microgels' size when the surfactant is in the *cis*-state. Figure 1(b) shows the theoretically calculated microgel size as a function of normalized surfactant concentration for two different values of the parameter ΔF describing surfactant hydrophobicity (Materials and Methods section). Higher values of ΔF correspond to a more hydrophobic surfactant, i.e., the curves calculated for $\Delta F = 15$ and $\Delta F = 8$ describe microgel swelling with *trans*- and *cis*-isomer, respectively. First, at small surfactant concentrations (up to 0.01 of CMC), the microgels are in a swollen state, while at larger concentrations [region I, Fig. 1(a), black line], the size of the microgels gradually decreases approaching its saturation value of almost half of the initial diameter at surfactant concentration of ca. 5% of the CMC. Depending on the charge density of the microgels and their concentration, the exact surfactant concentration at saturation varies, but the common trend is pursued. This effect was already reported in our previous

publication.¹⁸ In the concentrational range between 0.05 of CMC and 0.4 of CMC, the microgel is in a collapsed state [Fig. 1(a)]. However, when we increase the concentration of surfactant above the CMC [Fig. 1(a)], the microgels' size increases back to almost its initial value. At the CMC and higher, the microgel is in a swollen state with a diameter of 95% of its initial value.

In case when microgel interacts with *cis*-isomers [Fig. 1(a), red line], there is a similar tendency but shifted towards a larger absolute concentration. Indeed, the shrinkage of the microgel starts at 0.1 of CMC and saturates at 0.4 of CMC (region I), while above the CMC, the increase in the microgel size in the presence of the *cis*-isomer sets at 4 of CMC. Theoretically calculated curves plotted in Fig. 1(b) describe experimentally observed phenomena quite well. The collapse of the microgel (region I) is attributed to micellization of surfactants in the microgel interior resulting in a decrease of osmotic pressure as discussed in Refs. 19 and 20. The reswelling of microgels at high surfactant concentrations (black curve, Fig. 1) observed for the first time in this paper can be explained by the theoretical analysis of the system free energy presented in Materials and Methods section. Effective sorption of surfactants by microgel/surfactant complexes due to energy gain from micellization in the gel interior results in a considerable growth of the micellar phase, so that the total amount of surfactants trapped within the microgel exceed the total charge on microgel subchains. Thus, the charge reversal of microgels takes place (Fig. 2). Increase of microgel charge would have led to electrostatic energy enhancement that is not favorable. Thus, some part of surfactant counterions are forced to stay within microgels partially neutralizing their charge. Counterions' additional osmotic pressure provokes the microgel swelling at increasing surfactant concentrations. The higher the energy gain from micellization, i.e., the more hydrophobic the surfactant, the more effective its sorption by microgels. Thus, the neutralization of microgels with surfactant ions (accompanied by their precipitation, Fig. 1), further charge reversal as well as microgel reswelling shift to smaller surfactant concentrations at increasing surfactant hydrophobicity (increasing theoretical parameter ΔF or experimental *cis*- to *trans*-isomer switching).

Since one can switch reversibly between the *trans*- (black curve) and *cis*-state (red curve) by applying irradiation with UV and blue light, respectively, we rephrase the results presented in Fig. 1: at surfactant concentrations above the CMC,

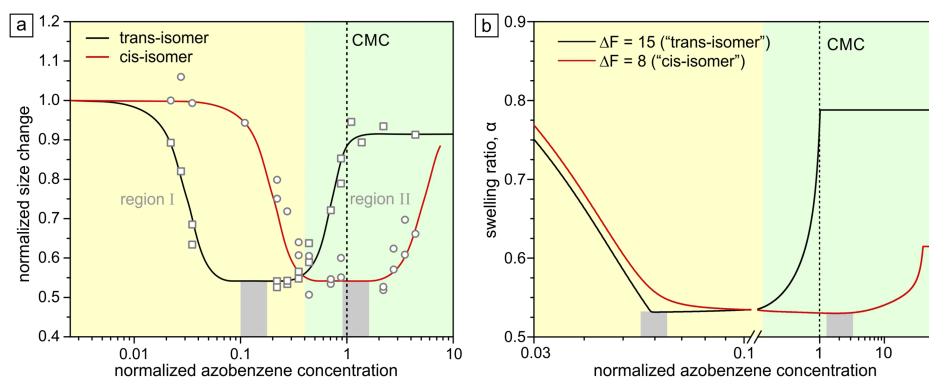


FIG. 1. (a) Dependence of the normalized diameter of the microgels on surfactant concentration: as measured experimentally. (b) Theoretically calculated swelling ratio α of the microgel as a function of normalized surfactant concentration at a different surfactant hydrophobicity ΔF .

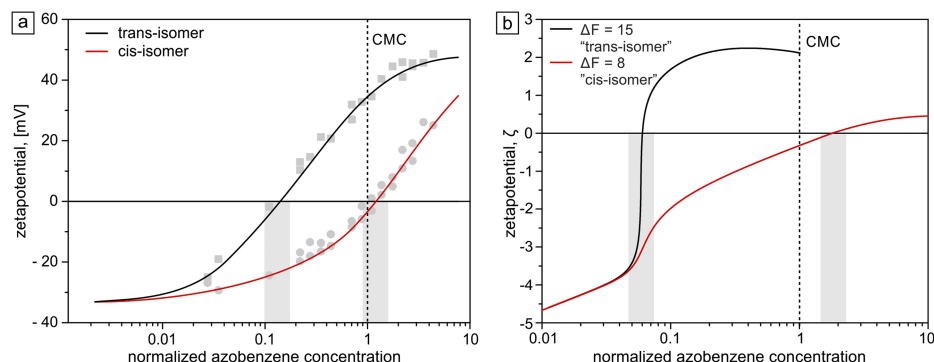


FIG. 2. (a) Zeta potential of the microgels in the presence of *trans*- (black curve) and *cis*-isomer (red curve) as a function of concentration expressed in terms of CMC. (b) Theoretically calculated zeta potential ζ as a function of normalized surfactant concentration at a different surfactant hydrophobicity ΔF . Normalization is performed with respect to CMC of more hydrophobic surfactant with $\Delta F = 15$.

the microgel is in a swollen state on blue irradiation and shrinks on UV irradiation (region II). While in the region I (below CMC), the microgels are in a collapsed state on blue irradiation and swollen during UV irradiation. At two particular absolute concentrations, 0.1 of CMC and CMC, the microgels precipitate out of solution, since at these concentrations the particles become neutral (Fig. 2). The precipitation at 0.1 of CMC takes place only in the case of *trans*-state of surfactant, while at CMC precipitation occurs for the *cis*-state. The shift of the precipitation region to smaller surfactant concentrations with increasing surfactant hydrophobicity is explained theoretically by a higher energy gain from micellization resulting in more effective surfactant sorption by microgel.

In both regions, the transition between swollen and collapsed states can be triggered by light in a reversible manner. At concentrations below the CMC (region I), on irradiation with UV light, the surfactant molecules desorbed out of the microgels resulting in the swelling of the particles back to their initial size. At a larger surfactant concentration (above the CMC, region II), the microgels shrink on UV irradiation and swell on blue irradiation, thus exhibiting opposite behaviour to region I (Fig. 3).

The kinetics of the size change in both regions is limited by a diffusion of the surfactant molecules in or out of the microgels. For microgel aggregates consisting of ca. 1000 particles, the swelling/deswelling takes place within first 10 s of irradiation (see the video in the [supplementary material](#),

Fig. S1). Scaling down to the size of the single microgel, one obtains 0.1 s for the size change. The inset in Fig. 3 shows three snapshots out of the video recorded in an optical microscope (Fig. S1) where the aggregate of the microgels was exposed periodically to irradiation with UV and blue light. The aggregate is formed by fast desolution of dried microgels.

In conclusion, we investigated complex formation of microgels with cationic azobenzene containing surfactant over the broad concentrational range starting far below and exceeding several times that of the CMC. We have found two regions where the microgels exhibit opposite behaviour on irradiation for two types of surfactant isomers. At small surfactant concentrations, the microgels shrink successively with concentrational increase of *trans*-isomers, while being in a swollen state in the presence of *cis*-isomer. At a larger surfactant concentration (exceeding CMC in solution), the microgels show reversed action: swelling in the presence of *trans*-isomers and shrinking on *cis*-isomers. Since the hydrophobicity of the photosensitive surfactant can be triggered by light and switched reversible between more hydrophobic (*trans*-isomer, blue light) and hydrophilic states (*cis*-isomer, UV irradiation), depending on the surfactant concentration, the microgels can be swollen either on UV or on blue irradiation. We also propose theoretical explanation of this phenomenon.

MATERIALS AND METHODS

Materials. Azobenzene containing surfactant with a spacer of six methylene groups between the positively charged trimethylammonium bromide head group and the azobenzene unit was synthesized as described elsewhere.²¹ The photoisomerization behavior of the surfactant is described in detail in previous publication.²² The *trans*-isomer has a characteristic absorption band with a maximum at 351 nm. The spectrum of the *cis*-isomer is characterized by two absorption bands with maxima at 313 nm and at 437 nm. The lifetime of the *cis*-isomer in the dark is 62 h, while the photo-isomerization from the *cis*-to *trans*-state under irradiation with blue light ($\lambda = 450$ nm, $I = 10$ mW/cm²) takes place within a few seconds, approaching a photo-stationary state after 10 min of irradiation.

Synthesis of the microgel. The microgel particles were synthesized as described elsewhere.²³ For this N-isopropylacrylamide (NIPAM, Aldrich, 97%), 5 mol. % (with respect to the mass of NIPAM) of

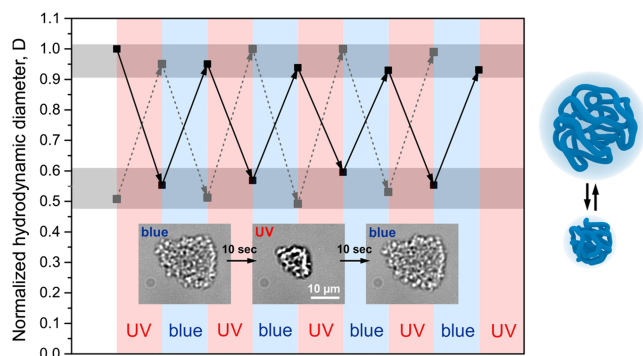


FIG. 3. Reversible changes of the hydrodynamic diameter under repeating UV and blue irradiation. Black line indicates the region II from the phase diagram in Fig. 1, and dashed line shows the region I. Inset shows three optical microscope snapshots of the microgel aggregate in the region II under exposure to UV and blue irradiation (see the video in the [supplementary material](#), Fig. S1).

N,N'-methylenebisacrylamide (BIS, Aldrich, 99,5%) and 50 mol. % of the co-monomer allyl acetic acid (AAA, Aldrich, 97%) were dissolved in 100 ml Milli-Q water, heated to 70 °C under a constant nitrogen stream. The polymerization was initiated by the addition of 1 mg KPS. After synthesis, the microgel was dialyzed for 14 days with Milli-Q water to remove oligomers and excess educts, and freeze-dried.

Sample preparation. The microgel and azobenzene containing surfactants were dissolved in de-ionized water (Milli-Q) and mixed together. The concentrations of surfactants were varied over a broad range starting from far below its CMC ($C_{CMC} = 0.5$ mM) and extending the CMC by several times, while the microgel concentration was kept fixed at $2 \cdot 10^{-5}$ M.

Dynamic light scattering (DLS) and zeta potential. Zeta potential and effective hydrodynamic radius measurements were carried out using a Zetasizer (Nano-ZS, Malvern Instruments, Ltd.) before and after irradiation.

Irradiation of the samples was performed during 10 minutes with either UV light ($\lambda = 365$ nm, $I = 9$ mW/cm², UV lamp: VL-4L, Fisher Scientific SAS) to induce *trans-cis* isomerization or with blue light ($\lambda = 450$ nm, $I = 10$ mW/cm², Conrad Electronic) to accelerate *cis-trans* isomerization.

Microscopy. Images were acquired with an Olympus XM10 monochrome camera at a speed of 1 frame/s using an inverted Olympus IX71 microscope. The solution of microgels was filled into a 400 μ m high microchannel (Ibidi μ slide VI 0.4), placed in the microscope, and irradiated periodically with UV and blue light during imaging.

Theoretical model

To describe the conformational behavior of microgel-surfactant solutions in a wide range of surfactant concentrations, we follow the theoretical approach developed in Refs. 19 and 20. In Ref. 20, we have considered microgel collapse at relatively low surfactant concentrations, while in the present work, we generalize the theory to analyze the phenomenon of microgel reswelling at high surfactant concentrations.

In our theoretical approach, the microgel is assumed to consist of ν flexible subchains each containing N monomer units of size a . Some fraction f of the monomer units is ionic. The equilibrium microgel size is defined through the microgel swelling ratio $\alpha = R/R_0$, which is the ratio between the equilibrium microgel radius R and the microgel radius R_0 in the reference Gaussian state. The average distance between the centers of adjacent microgels is defined as $2R_{out} = 2R_0/\gamma$ with a dimensionless parameter γ depending on microgel concentration, $\gamma \ll 1$ for diluted solutions. We denote as Z the number of surfactant molecules in the solution per one charged group on polymer subchains. Surfactants are oppositely charged with respect to the ionic monomer units.

The free energy of the solution per microgel can be written as a sum of the following terms:

$$F_{tot} = F_{el} + F_{int} + F_{el-st} + F_{tr}^{nc} + F_{tr}^s + F_{el-st}^{mic} + F_{tr}^{sc} + F_{agg},$$

where the first five terms, namely, the free energy F_{el} of elastic deformation of the microgel subchains within the framework of the Flory theory,²³ the free energy F_{int} of van der Waals' interactions of microgel monomer units in the form of the virial expansion, the Coulomb energy of charged microgels F_{el-st} ,

and the free energies of translational motion of microgel counterions F_{tr}^{nc} and free non-aggregated surfactant ions F_{tr}^s inside and outside microgels, remain unchanged; their expressions in the ideal gas approximation can be found elsewhere.^{19,20}

The term F_{el-st}^{mic} takes into account the Coulomb energy of micelles inside microgels. This contribution is negligible at low surfactant concentrations when the micellar charge is fully neutralized by microgel subchains but it starts to play a significant role when the total charge of surfactants absorbed by microgel exceeds the total charge on microgel subchains and the phenomenon of microgel charge reversal is observed. In this case, some fraction of surfactant counterions also takes part in micelle neutralization losing their translational entropy.

The Coulomb energy of charged micelles treated as the energy of a spherical capacitor reads

$$F_{el-st}^{mic} = N_{mic} \frac{Q_{mic}^2}{\epsilon} \left(\frac{1}{R_{mic}} - \frac{1}{R_{mic}^{out}} \right),$$

where ϵ is the relative dielectric permittivity of the solvent. The values $N_{mic} = \frac{N\nu f Z s q}{m}$, $R_{mic} = (mb^3 a^3)^{1/3}$, and $Q_{mic}/e = m \left(1 - \frac{1+Ztd}{Zsq} \right)$ are the number, radius, and charge of micelles, respectively, b being a surfactant length expressed in the monomer length units a , m being the micellar aggregation number, and $2R_{mic}^{out}$ is the average distance between neighboring micelles in the microgel interior. Values s and t denote the fractions of surfactant molecules and surfactant counterions, respectively, that are kept within the microgel.

The contribution F_{tr}^{sc} taking into account translational entropy of the surfactant counterions, which are regarded as an ideal gas both inside and outside the microgel, is written as

$$\frac{F_{tr}^{sc}}{k_B T} = Z f N \nu \left[t (1-d) \ln (Z t (1-d) f \Phi) + (1-t) \ln \left(\frac{Z (1-t) f \Phi \gamma^3}{\Phi N^{1/2} - \gamma^3} \right) + t d \left(\frac{N \nu Z t d f}{S_{mic} a} \right) \right].$$

Here $\Phi = \nu N a^3 / R^3$ is the polymer volume fraction inside the microgel. In this expression, the first two terms account for the entropy of mobile surfactant counterions inside and outside microgels, respectively. The last term is an entropic contribution from surfactant counterions condensed on charged micelles, and their fraction is denoted as d . We assume that these counterions are able to move in the outer layer of micelles with the total area $S_{mic} = R_{mic}^2 N_{mic} = N \nu f Z s q b^2$.

Finally, the last term F_{agg} is aggregation free energy responsible for surfactant micellization. If we denote the fraction of aggregated surfactant molecules within the microgel as q , then

$$\frac{F_{agg}}{k_B T} = N \nu Z f s \left[(1-q) \ln (1-q) + \frac{q}{m} \ln (q) - q \frac{m-1}{m} \ln \left(\frac{Z s f \Phi}{exp} \right) - q \Delta F \right],$$

where ΔF is the energy gain per surfactant ion due to micellization.

The free energy function $F_{tot}(\Phi, \beta, s, t, q, d)$ was minimized with respect to six variables to find out the equilibrium microgel state. The resulting equations correspond to the

equality of chemical potentials of all system components inside and outside the microgel and equality of the corresponding osmotic pressures. The calculations were performed for the following values of the system parameters: $\nu = 10^8$, $N = 15$, $f = 0.33$, $\gamma = 0.05$, $e^2/\epsilon a k_B T = 1$, $b = 2$, and theta-solvent for microgel subchains. The aggregation number m was chosen to be 50, which is typical for spherical micelles. In fact, the exact numerical value of $m \gg 1$ hardly influences theoretical conclusions. For further comparison of theoretical results with experimental data, the swelling ratio is recalculated with respect to the microgel radius in the swollen state realized in surfactant-free solution [Fig. 1(b)]. ζ -potential is calculated as $\zeta = Q/\epsilon R$, where $Q = e\nu N f(1 - \beta + sZ - tZ)$ is an uncompensated microgel charge [Fig. 2(b)], where β is the fraction of network counterions that are kept within the microgel.

SUPPLEMENTARY MATERIAL

See [supplementary material](#) for the video of the reversibly swelling microgel particle shown in Fig. S1.

ACKNOWLEDGMENTS

This research is supported by the International Max Planck Research School on Multiscale Bio-Systems, Potsdam, German-Russian Interdisciplinary Science Center, Germany and Russian Foundation for Basic Research. R.v.K. acknowledges the DFG for financial support (KL 1165/12). We thank Dr. Kopyshchev for fruitful discussions and graphical support.

¹A.-L. M. Le Ny and C. T. Lee, *J. Am. Chem. Soc.* **128**, 6400 (2006).

²M. Sollogoub, S. Guieu, M. Geoffroy, A. Yamada, A. Estévez-Torres, K. Yoshikawa, and D. Baigl, *ChemBioChem* **9**, 1201 (2008).

³A. A. Zinchenko, M. Tanahashi, and S. Murata, *ChemBioChem* **13**, 105 (2012).

⁴S. Rudiuk, K. Yoshikawa, and D. Baigl, *Soft Matter* **7**, 5854 (2011).

⁵Y. Zakrevskyy, P. Cywinski, M. Cywinska, J. Paasche, N. Lomadze, O. Reich, H.-G. Löhmansröben, and S. Santer, *J. Chem. Phys.* **140**, 044907 (2014).

⁶L. Lysyakova, N. Lomadze, D. Neher, K. Maximova, A. V. Kabashin, and S. Santer, *J. Phys. Chem. C* **119**, 3762 (2015).

⁷A. Kopyshchev, C. J. Galvin, J. Genzer, N. Lomadze, and S. Santer, *Langmuir* **29**, 13967 (2013).

⁸A. Kopyshchev, C. J. Galvin, R. R. Patil, J. Genzer, N. Lomadze, D. Feldmann, J. Zakrevski, and S. Santer, *ACS Appl. Mater. Interfaces* **8**, 19175 (2016).

⁹D. Feldmann, S. R. Maduar, M. Santer, N. Lomadze, O. I. Vinogradova, and S. Santer, *Sci. Rep.* **6**, 36443 (2016).

¹⁰A. Venancio-Marques, F. Barbaud, and D. Baigl, *J. Am. Chem. Soc.* **135**, 3218 (2013).

¹¹D. Baigl, *Lab Chip* **12**, 3637 (2012).

¹²A. Diguët, H. Li, N. Queyriaux, Y. Chen, and D. Baigl, *Lab Chip* **11**, 2666 (2011).

¹³A. Diguët, R.-M. Guillemic, N. Magome, A. Saint-Jalmes, Y. Chen, K. Yoshikawa, and D. Baigl, *Angew. Chem., Int. Ed.* **48**, 9281 (2009).

¹⁴S. N. Varanakkottu, S. D. George, T. Baier, S. Hardt, M. Ewald, and M. Biesalski, *Angew. Chem., Int. Ed. Engl.* **52**, 7291 (2013).

¹⁵T. Hayashita, T. Kurosawa, T. Miyata, K. Tanaka, and M. Igawa, *Colloid Polym. Sci.* **272**, 1611 (1994).

¹⁶Y. Zakrevskyy, M. Richter, S. Zakrevska, N. Lomadze, R. von Klitzing, and S. Santer, *Adv. Funct. Mater.* **22**, 5000 (2012).

¹⁷M. Richter, Y. Zakrevskyy, M. Eisele, N. Lomadze, S. Santer, and R. von Klitzing, *Polymer* **55**, 6513 (2014).

¹⁸S. Schimka, N. Lomadze, M. Rabe, A. Kopyshchev, M. Lehmann, R. von Klitzing, A. M. Romyantsev, E. Y. Kramarenko, and S. Santer, *Phys. Chem. Chem. Phys.* **19**, 108 (2017).

¹⁹A. M. Romyantsev, S. Santer, and E. Y. Kramarenko, *Macromolecules* **47**, 5388 (2014).

²⁰A. R. Khokhlov, E. Y. Kramarenko, E. E. Makhaeva, and S. G. Starodubtzev, *Die Makromol. Chem., Theory Simul.* **1**, 105 (1992).

²¹D. Dumont, T. V. Galstian, S. Senkow, and A. M. Ritcey, *Mol. Cryst. Liq. Cryst.* **375**, 341 (2002).

²²Y. Zakrevskyy, J. Roxlau, G. Brezesinski, N. Lomadze, and S. Santer, *J. Chem. Phys.* **140**, 044906 (2014).

²³A. Y. Grosberg and A. R. Khokhlov, *Statistical Physics of Macromolecules* (Nauka Publishers, Moscow, 1989) [(AIP Press, New York, 1994) (in English)].